

Garnet-quartz intergrowths in graphitic pelites: the role of the fluid phase

KEVIN W. BURTON*

Department of Geological Sciences, University College London, Gower Street, London WC1E 6BT, UK

ABSTRACT. Garnets with an unusual inclusion pattern of cylindrical quartz intergrowths have been found to develop exclusively in the presence of graphite. The intergrowths consist of quartz rods, 1-5 μm in diameter, originating at the sector-zone interfaces in the garnet with the long axes normal to the crystal faces. The lattice orientation and continuity of the quartz suggests that the interphase boundaries between the quartz and garnet are epitaxially related and that new material was added to the tube as the crystal face of the garnet grew. In the presence of a C-O-H fluid, at the temperatures and pressures recorded, ($P = 6.5$ kbar, $T = 500$ °C), the amount of CO_2 present restricts the solubility of SiO_2 in the intergranular fluid phase, where the oxygen fugacity (f_{O_2}) is below the Quartz-fayalite-magnetite (QFM) buffer, and within the stability field of graphite. The reduced solubility will lower the concentration of SiO_2 in solution, and hence restrict its ease of transport via the fluid, resulting in an excess of SiO_2 at the site of garnet growth. Under such conditions the SiO_2 is incorporated in the growing garnet in the form of the cylindrical quartz intergrowths.

KEYWORDS: garnet, quartz, intergrowths, graphitic pelites.

GARNETS in graphitic pelites sometimes develop a radial structure of quartz intergrowths. These garnets also show a cross-type inclusion pattern analogous to that observed in chistolite, and have been observed in both regional and contact metamorphic terrains (Harker, 1939; Henley, 1970; Novak and Holdaway, 1981; Andersen, 1984; Billet, 1984). Harker (1939) attributed the inclusion pattern to the development of twinning under conditions of rapid growth, whilst Andersen (1984), who also argued that the inclusion pattern was the result of rapid growth, considered the quartz intergrowths to be the result of a cellular solidification mechanism.

Graphite is commonly reported in rocks containing such garnets, as is the case in the examples discussed here. Inspection of the Harker thin-section collection at Cambridge confirmed that,

* Present address: Department of Earth Sciences, University of Cambridge, Downing Street, Cambridge CB2 3EQ.

without exception, such garnets are always characterized by the presence of graphite. The presence of graphite in pelitic rocks will control the oxygen fugacity (f_{O_2}), (Miyashiro, 1964; French, 1966; Ohmoto and Kerrick, 1977; and Frost, 1979). The graphite exerts a buffering function which effectively maintains low oxidation states as long as it is present and able to react with the fluid phase.

The key example discussed in this study is an upper-amphibolite facies pelite, in which graphite-bearing and graphite-free laminae less than 1 cm across, having different oxidation states, have been preserved during metamorphism (cf. Chinner, 1960; Rumble, 1978), thus preserving local gradients of f_{O_2} on a scale of micrometres. Garnets containing the quartz intergrowths are restricted to the graphite-bearing layers. In the light of this unique association with graphite, the present study focuses on the development of the quartz intergrowths in an attempt to determine the likely growth mechanism and physical conditions of metamorphism responsible for their occurrence.

Inclusion and intergrowth geometries

Inclusion and intergrowth patterns in the garnets may be divided into two categories following Andersen's (1984) classification, according to their shape and orientation and with respect to the crystallography of the garnet host (see fig. 1a, b, c, d).

Type 1 inclusions are concentrated along growth sector boundaries, parallel to the $\{110\}$ crystallographic planes. These boundaries define the trace of the intersection surface between two adjacent $\{110\}$ crystal faces as they grew from the garnet centre. Individual inclusions defining this pattern are predominantly equidimensional, and irregular, but often elongate parallel to the $[110]$ direction. Where identification is possible inclusions are found to consist of quartz, ilmenite and graphite. That the inclusions represent relicts of the matrix is sometimes suggested by their gradual coarsening

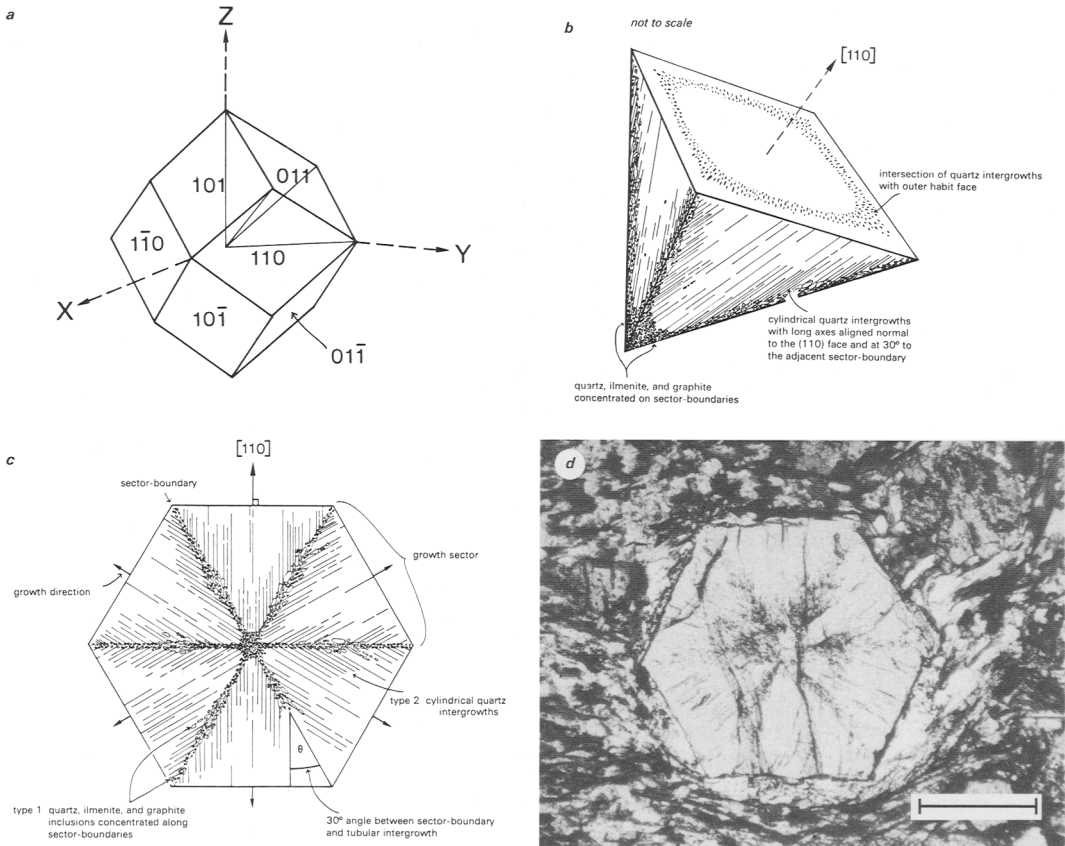


FIG. 1. (a) External morphology of a rhombododecahedral garnet crystal bounded by $\{110\}$ crystal faces. (b) Schematic growth pyramid of garnet, showing inclusion and intergrowth geometry. Synoptically the garnet is made up of twelve such pyramids, with common apices at the centre of the crystal and bases formed by the $\{110\}$ crystal faces. (c) Sketch section through garnet centre showing the relationship of the inclusion and intergrowth pattern to the crystallography of the garnet host. (d) Photomicrograph of garnet porphyroblast sectioned through the centre. Scale bar approx. $500 \mu\text{m}$.

towards the margins of the garnets, an indication of prograde coarsening of the matrix.

Type 2 are long, cylindrical quartz intergrowths $1\text{--}5 \mu\text{m}$ in diameter which unlike the inclusions concentrated on the sector boundary planes, are not relicts of the matrix, but were formed simultaneously with the growing garnet. They originate at the sector boundaries with the long axes normal to the $\{110\}$ crystal faces, aligned in the $[110]$ direction. Although the majority of these tubular intergrowths are orientated at an angle of 30° to the sector-boundaries, in some garnets the tubes show a strong curvature. The intergrowths have a circular cross-section seen in sections cut parallel to crystal faces. They usually have a constant diameter from origin to closure, but in some cases widen towards the outer face of the crystal, from 1 up to $40 \mu\text{m}$, giving rise to a trumpet-like form. Each

intergrowth has a uniform extinction, demonstrating that the crystal lattice is continuous. However, variations in extinction direction from one inclusion to another indicate a random orientation of the quartz lattice relative to the garnet lattice. The absence of a preferred lattice orientation of the intergrowths relative to garnet, indicates that the interphase boundaries between the quartz and garnet are non-coherent. The lattice continuity of the quartz shows that new material was added to the end of the intergrowth as the crystal face of the garnet grew.

Sample petrography

The key sample discussed here is from the Skaiti Supergroup in the Caledonian metamorphic terrain of the Sulitjelma copper mining district,

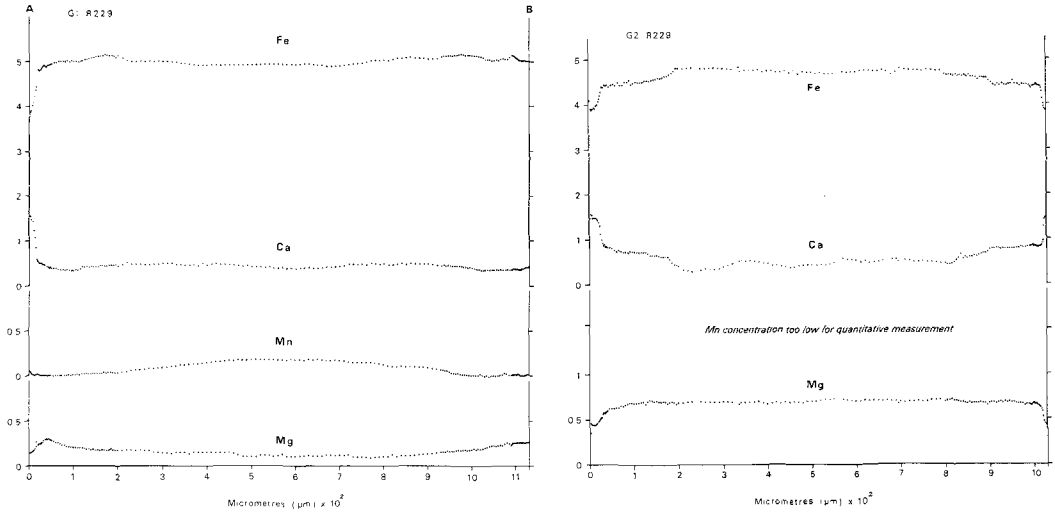


FIG. 2. (a, left) Garnet zoning profile for garnet G1-R229 from the graphite-bearing assemblage. (b, right) Garnet zoning profile for garnet G2-R229 from the graphite-free assemblage. Profiles plotted in cations per formula unit based on 24 oxygens. dots = analysis points with intervals of 2, 5, 10, and 20 μm .

North Norway (67° N., 16° E.). These rocks, considered to represent continental crust on one side of the Sulitjelma ophiolite complex (Boyle *et al.*, 1985), underwent metamorphism prior to ophiolite emplacement during the Caledonian orogeny.

The sample is heterogeneous on a millimetre scale, partly because of original sedimentary lithological layering on this scale (i.e. those layers with and without graphite), and as a result of this, partly because of the variable nature and extent of reaction within each layer. Accordingly the mineral assemblages may be divided into two groups: (1) graphite-bearing and (2) graphite-free. Garnets containing the quartz intergrowths are confined to the graphite-bearing layers. They are idioblastic, up to 1.5 mm in diameter, and display a concentric chemical zonation. The zoning is characterized by a barely discernible but nevertheless distinct decrease in Mn from core to rim, with an antipathetic variation in Fe, shown in fig. 2a. This is consistent with the more typical bell-shaped Mn profile (see Hollister, 1969; Loomis, 1982) attributed to continuous reaction during growth at low grades, with or without subsequent diffusional homogenization (Woodsworth, 1977; Yardley, 1977). Many of the garnets have a partially developed outer rim, in which graphite is abundant, but there are no quartz intergrowths or sector-boundary inclusions. There is a corresponding change in composition at this rim (see rim marked A fig. 2a) with Fe and Mg decreasing sharply and Ca increasing. Where this

outer rim is not developed (for example rim B fig. 2a) a thin partial corona of quartz is commonly present enveloping the inner rim.

In addition to the concentric chemical zonation the garnets are sometimes characterized by a radial zoning, related to the intergrowth pattern. Adjacent to the quartz intergrowths a chemical zoning profile is often superimposed on the overall zoning. There is an increase in Mn and Ca, and a decrease in Fe and Mg, towards each intergrowth as shown in fig. 3. However, not all of the intergrowths have this associated compositional variation, suggesting that the zoning is not an essential condition for their development. Rather such localized zoning is thought to have developed as a consequence of diffusion subsequent to intergrowth formation.

In contrast, the garnets in the graphite-free layers have a skeletal anhedral to subhedral shape, up to 1 mm in diameter and are often elongate parallel to the schistosity. They do not contain the quartz intergrowths or sector boundary inclusions and have randomly orientated inclusions comprising of most of the matrix phases. The garnets are chemically zoned, although such zoning is quite unlike that observed in the garnets in the graphite-bearing assemblage, see fig. 2b. Mn is not detectable at any point in the profile and Fe and Mg show an irregular decrease from core to rim, whilst Ca increases. Interestingly the rim composition of garnets in the graphite-free assemblage and outer rim composition of garnets in the graphite-bearing assemblage are identical.

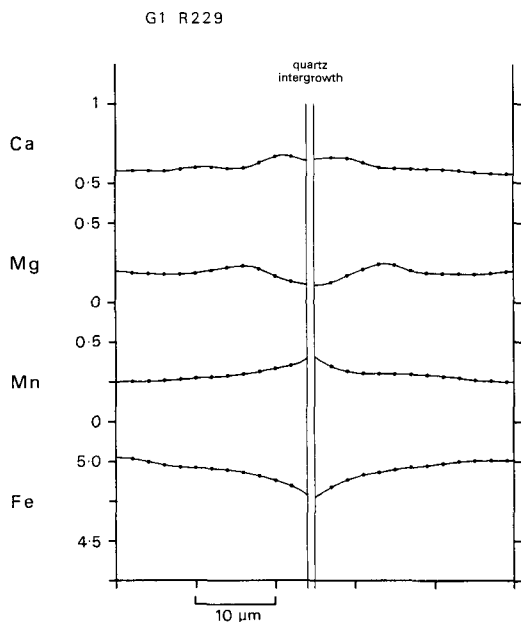


FIG. 3. Typical example of the chemical zoning profile sometimes developed adjacent to the quartz intergrowths. Profiles plotted in cations per formula unit based on 24 oxygens.

The control that graphite exerts on both the textural and compositional development of garnet is strikingly demonstrated in the case of one garnet which has actually grown across the boundary between the two assemblages. The garnet, shown in fig. 4, has been contoured for Fe, Mg, Mn, and Ca. The part of the garnet located in the graphite-bearing assemblage is idioblastic with well-developed quartz intergrowths and inclusions concentrated on the sector-boundaries, whilst the chemical zoning pattern is similar to that observed in other garnets in the graphite-bearing assemblage. In an interval of less than $100\ \mu\text{m}$ across the assemblage boundary, there is a dramatic change in both textural and compositional development. The quartz intergrowths and sector-boundary inclusions are absent and the outer rim of the garnet is poorly developed, whilst the chemical zoning is similar to garnets in the graphite-free assemblage, providing compelling evidence that graphite is capable of buffering fluid and mineral compositions on a length scale less than the diameter of an individual crystal, i.e. a scale of micrometres.

Finally, there is a marked contrast in the grain size of matrix minerals common to both assemblages. The graphite-bearing assemblage is characterized by a very small grain size, for ex-

ample, the average grain size of quartz is $< 0.1\ \text{mm}$, whereas in the graphite-free assemblage the grain size of quartz is usually $> 0.3\ \text{mm}$, although the modal abundance of minerals in each assemblage is similar.

Conditions of metamorphism

Geothermometry and geobarometry. On the scale of a single thin-section it is reasonable to assume that both assemblages in sample R229 were subject to the same temperature and pressure conditions during metamorphism. Temperature was determined using the garnet-biotite geothermometer of Ferry and Spear (1978) using the modifications of Hodges and Spear (1982), and pressure was determined using the plagioclase-biotite-garnet-muscovite geobarometer of Ghent and Stout (1981).

Two estimates were made for the garnets in the graphite-bearing assemblage. The first uses the inner garnet rims, which represent the composition and point beyond which the quartz intergrowths do not extend. The second uses the composition of the outer rim, where it is present. In the case of the outer rim, retrograde cation exchange between the garnet and adjacent biotites precludes their use in assessment of the peak metamorphic equilibrium compositions. However, assuming that equilibrium once extended further throughout the matrix, the use of biotite and garnet compositions not in contact may provide a reasonable constraint on P - T conditions. The first estimate uses the core composition of plagioclase whereas the second uses the rim. Muscovite compositions are relatively constant and are considered unlikely to affect the Fe-Mg exchange equilibria markedly.

Results were consistent throughout the sample and show that the compositions represented by the inner rims of the garnets in the graphite-bearing assemblage correspond to a maximum temperature of $500 \pm 20\ ^\circ\text{C}$ and a pressure of $6.5 \pm 0.8\ \text{kbars}$, and the outer rim corresponds to a temperature of $600 \pm 25\ ^\circ\text{C}$ and pressure of $8.5\ \text{kbars} \pm 1\ \text{kbar}$. A single estimate was made for the garnets in the graphite-free assemblage using rim compositions of all minerals and this gave temperatures of $600 \pm 25\ ^\circ\text{C}$ and pressures of $8.5\ \text{kbars}$ in good agreement with the outer rims in the graphite-bearing assemblage. The presence of biotite as an included phase in the cores of the garnets in the graphite-free assemblage enabled a determination of core temperatures, found to be $520 \pm 20\ ^\circ\text{C}$.

Calculation of fluid compositions. Many authors have shown (Eugster, 1959; French, 1966; Ohmoto and Kerrick, 1977; Frost, 1979) that in the presence of graphite the composition of the fluid phase may

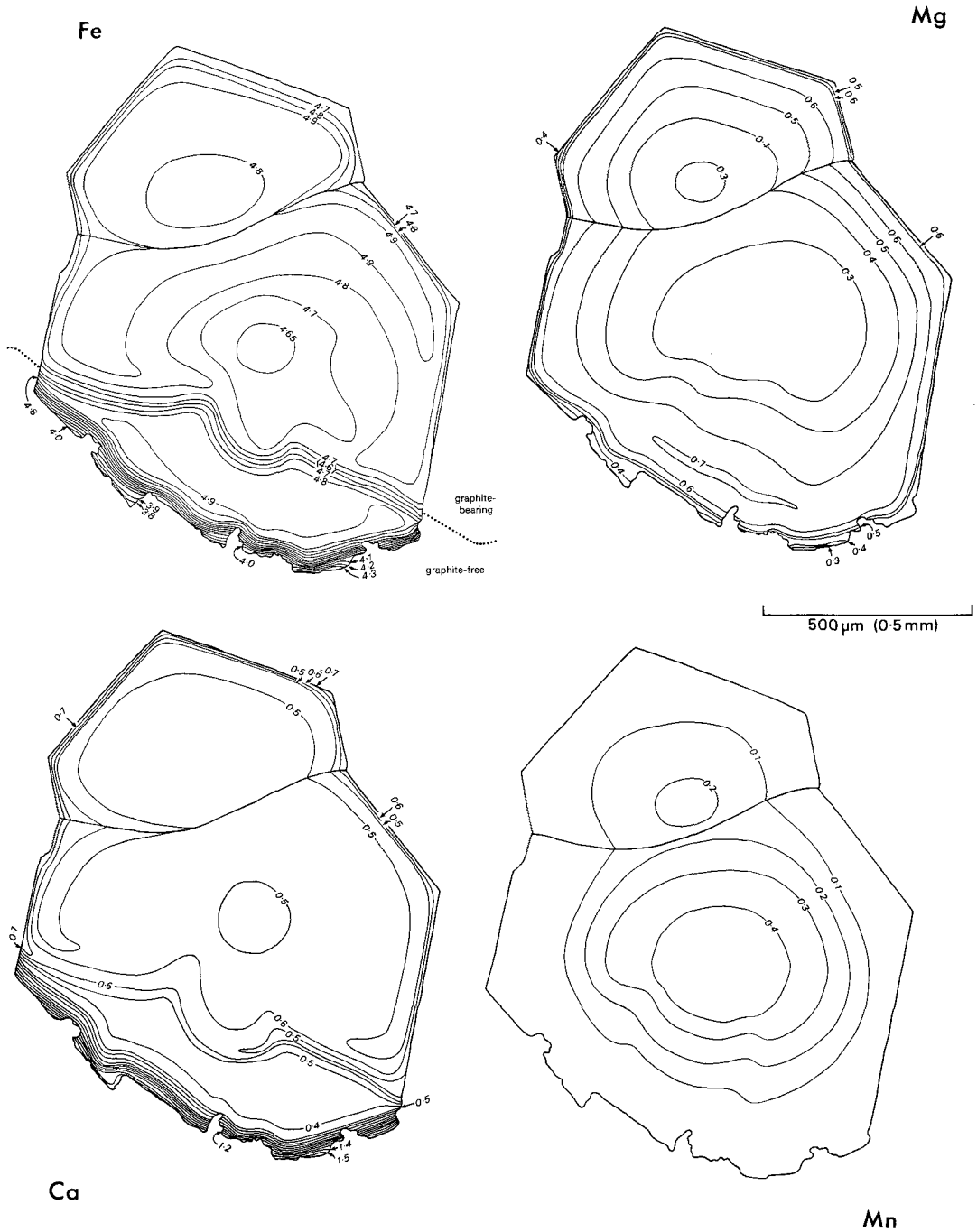
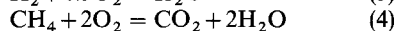
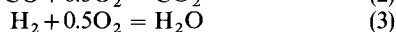
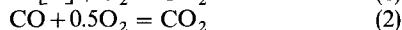
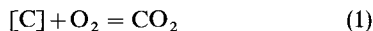


FIG. 4. Zoning maps of garnet G3-R229, which straddles the boundary between graphite-bearing and graphite-free assemblages. Contoured for Fe, Mg, Ca, and Mn, and plotted in cations per formula unit based on 24 oxygens.

depart substantially from pure H₂O. Fluids can contain significant proportions of other volatiles in the C-O-H system. Calculations have demonstrated that there are six important fluid species, namely H₂O, CO₂, CH₄, CO, H₂, and O₂. At a known pressure (*P*) and temperature (*T*) the composition of the fluid that coexists with graphite can be specified through four independent equilibria (Ohmoto and Kerrick, 1977; Lamb and Valley, 1984):



There are eight variables in this system, the six fluid species; the fluid-pressure (*P_f*); and the activity of graphite (*a_C*). If a fluid phase is present in a graphite-bearing system (where *a_C* = 1), by assuming that *P_{Fluid}* = *P_{Lithostatic}*, it is possible to calculate the fugacity of five fluid species by determining the fugacity of one. Consequently, following the phase rule, the state of a three-component fluid in equilibrium with graphite can be computed as functions of three intensive variables *T*, *P*, and *f_{O₂}*. The latter is an independent variable, and thus at fixed *P* and *T* fluid compositions can be calculated for a series of independently determined values of *f_{O₂}*.

Coexisting Fe-Ti oxides have been successfully used to estimate *f_{O₂}* and temperature in a wide range of metamorphic terrains. Ilmenite, and more rarely, magnetite, are found in the graphite-bearing assemblage, but there is no unique solution for *f_{O₂}* and *T* using the method of Buddington and Lindsley (1964), because the magnetite is virtually pure Fe₃O₄. However, given the composition of ilmenite, both from the matrix and as an included phase in garnet, and using the temperature determined by standard geothermometry (Ferry and Spear, 1978), it is possible to estimate a maximum value for the oxygen fugacity. By comparison with Fig. 5 of Buddington and Lindsley (1964, p. 316) the composition of ilmenite found as an inclusion in garnet corresponds to a value of log *f_{O₂}* bars = -22.8 at 500 °C and, for matrix ilmenite, -21.00 at 600 °C, the temperature estimated for the inner and outer garnet rims in the graphite-bearing assemblage. Given that dehydration reactions, such as the garnet forming reaction, will tend to drive *X_{H₂O}* to its maximum value (Ohmoto and Kerrick, 1977), the value of *f_{O₂}* determined for the outer garnet rims does not seem unreasonable. By contrast, the composition of magnetite, almost pure Fe₃O₄, in the graphite-free assemblage corresponds to a minimum value of log *f_{O₂}* bars = -18.8 bars at 525 °C. This suggests a difference of some four orders of magnitude over a length scale of a few micro-

metres between the two assemblages. Unfortunately, in the absence of graphite, where *a_C* is unknown, it is not possible to calculate the composition of the coexisting fluid phase and in this case the presence of an essentially H₂O dominated fluid is assumed.

Fluid compositions for the graphite-bearing assemblage were computed using a modified hard-sphere Redlich-Kwong equation of state, Holloway (1981), and ideal mixing of the fluid was assumed.

Table 1.

Physical conditions of metamorphism during garnet growth and molar proportions of fluid constituents estimated for the graphite-bearing assemblage.

	inner rim	outer rim
T (Deg C)	500	600
P (bars)	6500	8500
log <i>f</i> (O ₂) (bars)	-22.8	-21.0
<i>X</i> (CO ₂)	4.83E-01	2.94E-02
<i>X</i> (CH ₄)	1.08E-03	6.29E-02
<i>X</i> (H ₂ O)	5.15E-01	9.06E-01
<i>X</i> (CO)	1.32E-04	6.02E-05
<i>X</i> (H ₂)	1.82E-04	1.95E-03

Results of these calculations are shown as a function of *f_{O₂}* at a constant *P* and *T* (Table 1). These calculations show that in the case of the inner rim, which approximates most closely the conditions under which the quartz intergrowths developed, the main constituents of the fluid were H₂O, CO₂, and CH₄, in the approximate proportions *X_{H₂O}* = 0.515, *X_{CO₂}* = 0.483 and *X_{CH₄}* = 0.001.

Growth Models

Three hypotheses are advanced which might account for the growth of the cylindrical quartz intergrowths.

(1) The cellular solidification model (Andersen, 1984). Cellular solidification is commonly observed in metals (Chalmers, 1964; Rutter and Chalmers, 1965; Porter and Easterling, 1981). Such structures arise when thermal gradients in the matrix cause the growth face to become unstable and break down to a close packed array of cellular projections. In this case the intergrowths would have originated at the site of the narrow channels between the cellular projections. At still lower temperature gradients the cellular projections may develop secondary arms (i.e. dendritic growth takes place).

(2) The symplectite growth model (Spry, 1969). This is analogous to cellular precipitation in

metals (Porter and Easterling, 1981). This hypothesis proposes that the intergrowths grow simultaneously and co-operatively with the garnet behind a planar growth front. In contrast to the cellular solidification model, there is no primary irregularity at the growth front. Rather, the crystallization of two solid phases develops from a single parent phase (i.e. liquid \rightarrow garnet + quartz).

(3) The dislocation growth model (Burton *et al.*, 1951; Frank, 1951). In this case each cylindrical intergrowth represents the hollow core of a growth spiral associated with a giant screw dislocation (or number of smaller dislocations). These are known to develop in order to minimize the enormous strain energy near the core of such a large dislocation.

Cellular solidification was favoured by Andersen (1984), but whilst accounting for the morphology of the intergrowths parallel to the [110] direction, it does not account for their shape normal to this direction. In cellular growth the narrow channels between the cellular projections develop as a series of interconnected grooves dissecting the crystal face, rather than the isolated cylindrical tubes observed in the case of the garnets (see Rutter, 1958, p. 243, which shows the external interface of a cellularly solidified alloy). Further, according to the cellular growth hypothesis such channels are thought to develop as depressions in the growth front. Given that garnet preferentially fractionates manganese, a decrease in that element would be expected to occur adjacent to the intergrowths, as opposed to the increase sometimes observed, see fig. 3. Moreover, the model takes no account of the ubiquitous presence of graphite.

Thus the two alternative hypotheses, 2 and 3 above, presented in this study are preferred, although they are not necessarily independent, as symplectic intergrowths often develop preferentially on the sites of dislocations. Clearly any favoured model must account for both the intergrowth morphology and the characteristic presence of graphite, and thus C-O-H fluid equilibria.

The dilution of H₂O by significant proportions of CO₂ has a marked effect on the solubilities of minerals. Although data are scarce, experimental determinations of the solubility of SiO₂ in H₂O-CO₂ mixtures (Shettel, 1973; Novgorodov, 1975; Walther and Orville, 1983) suggest that, at the X_{CO_2} values determined here, the solubility of SiO₂ will be substantially lower than that for pure H₂O. Thus the concentration of SiO₂ in solution will be lowered and the ease of transport of SiO₂ via the intergranular fluid phase will be decreased. In a pure H₂O fluid system any excess components at the site of crystallization will be incorporated into the fluid phase to be transported and precipitated

at more favourable sites of growth, lowering the free energy and thereby re-establishing chemical equilibrium in the system. However, in CO₂ rich fluids the transport of SiO₂ is severely restricted and it is therefore incorporated in the growing garnet in the form of the cylindrical quartz intergrowths.

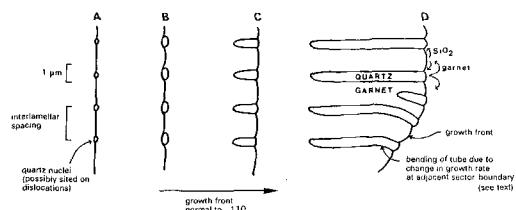


FIG. 5. Schematic diagram showing a possible sequence of steps during the development of the cylindrical quartz intergrowths.

Fig. 5 shows how two phases can grow co-operatively and simultaneously behind an essentially planar crystallization front. As the garnet grows, excess SiO₂ diffuses a short distance laterally, where it is precipitated on the quartz tubes. The rate at which the garnet grows will depend on how fast this grain boundary diffusion can occur and this in turn will depend on the spacing of the quartz intergrowths. Thus smaller spacings between adjacent intergrowths should result from more rapid growth. There will, however, be a lower limit to the spacing determined by the need to supply the garnet-quartz interfacial energy. The spacing will also be dependent on the amount of temperature overstep of the garnet-forming reaction (Porter and Easterling, 1981).

In this context, the marked decrease in grain size of matrix minerals, especially quartz, in the graphite-bearing assemblage compared to the graphite-free assemblage, is thought to reflect a decrease in solubility in the presence of graphite, which would then impair the usual prograde coarsening of matrix minerals (Spry, 1969).

The straight growth direction of the intergrowths, normal to the {110} crystal faces, results from a tendency to minimize the free energy of the system. Such an orientation is favoured since any bending would increase the free energy per unit length of intergrowth. Therefore, it follows that if the direction of growth is due to a crystallographic control, aligning the tube normal to the growth front, any bending must be due to a change in the direction of that growth front. The intergrowths curve either towards, or away from, the adjacent

sector boundary, but always as a mirror image to those in the opposite sector. This pattern is not consistent with any sort of physical external control, such as rotation of the garnet during growth. As an alternative, if the intergrowths are sited on, or influenced by, growth dislocations then the bending may be due to other factors, such as (1) changes in the stress field due to a sudden change in composition, leading to another preferred direction of minimum energy (van Enckevort *et al.*, 1982), or (2) macroscopically high growth steps sweeping over the growth face influencing the path of dislocations (Klapper, 1980).

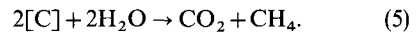
Discussion

The low concentration of elements in solution and restricted transport should in general lead to larger oversteps in reaction temperatures (Walther and Wood, 1984). However, in this study any tendency towards overstepping appears to have been counteracted by the effect of CO₂ on equilibria involving H₂O. Greenwood (1967) and Kerrick (1974) have demonstrated that, in the presence of CO₂, the temperature of dehydration equilibria, such as the garnet-forming reaction, will be lowered. This accounts for the lower temperatures recorded by the inner rims of the garnets in the graphite-bearing assemblage, as well as the presence of manganese in these garnets (Mn being undetectable in the garnets in the graphite-free assemblage). Carmichael (1970) reports a similar occurrence in a thin graphite-bearing pelite in the Whetstone Lake area, Ontario, where a Ca-rich amphibole has grown at unusually low temperatures. The observation also suggests that during nucleation and growth the garnet-forming components are readily available within the immediate few micrometres and do not need to be transported any great distance. If local diffusion controlled growth, competition for components would restrict the growth rate of neighbouring crystals. This is clearly not the case in the graphite-bearing assemblage, as garnets commonly develop in close proximity to neighbouring crystals, and in many instances the adjacent crystallization fronts intersected during growth but the two crystals continued to grow apparently unaffected, as is the case in garnet G3-R229 (see fig. 4). Fisher (1978) demonstrated that if crystals are closely spaced relative to the ability of diffusion or fluid flow to transport components, the growth rate must be controlled by interface kinetics or equilibrium. The general lack of inclusions in the garnets in the graphite-bearing assemblage (in contrast to those in the graphite-free assemblage) would imply slow growth rates. The quartz intergrowths in these

garnets attest to the fact that any matrix quartz in the vicinity was involved in the garnet-forming reaction, and where in excess was reprecipitated. The well developed {110} crystal faces also indicate slow growth (Sprey, 1969), probably close to equilibrium. However, the well developed crystal faces also indicate that interface control influenced the rate of growth. Thus it is concluded that the growth rate was controlled by interface kinetics, close to equilibrium.

Apart from graphite fluid equilibria and dehydration reactions, other oxidation-reduction equilibria may affect the oxygen fugacity, and hence affect fluid composition during prograde metamorphism. In particular, equilibria involving magnetite, or Fe³⁺ in solution, in ilmenite or Fe-Al silicates, and its reduction to Fe²⁺. The rarity of magnetite in the graphitic assemblage suggests that the buffering capacity of these equilibria is usually overridden by graphite fluid equilibria. A possible reason for this is the low molar volume of graphite (French, 1966). Where magnetite does occur in the graphite-bearing assemblage of sample R229, there is some evidence of localized buffering. For example, chlorite is only found as an intergrowth with, or rimming, magnetite, and where magnetite occurs as an included phase in garnet it locally affects the garnet composition as well as preventing the formation of the quartz intergrowths, thus indicating that it is exerting an oxidizing effect (buffering f_{O_2} to higher values) in the local domain of equilibrium.

Where the system is internally buffered, low temperature dehydration reactions will tend to drive X_{H_2O} to its maximum value. This in turn will cause the carbon content and H₂O to decrease continuously due to the reaction:



The maintenance of maximum X_{H_2O} results from the production of equal proportions of CO₂ and CH₄, (Ohmoto and Kerrick, 1977). Therefore one would expect the graphite content to decrease continuously during prograde metamorphism, but whilst graphite is present f_{O_2} will be kept low irrespective of f_{CO_2} or f_{CH_4} .

Internal control or buffering of the fluid composition by graphite, would suggest that the chemical potential of SiO₂ was also internally controlled (as a J-component according to Thompson, 1970). Thus, the development of the quartz intergrowths may serve as an indicator of changes in fluid composition during metamorphism. Such changes may be brought about by: (1) changes in the intensive variables P , T , and f_{O_2} , for example, as pressure increases max. X_{H_2O} increases greatly, such that at 10 kbars max. $X_{H_2O} = 0.99$. This is because the fugacity coefficient of H₂O remains around 1.0

even at high pressures, whereas the fugacity coefficient for CO_2 increases greatly with increasing pressure, (Skippen, 1977). The effect is amplified further by non-ideality of the fluid (Frost, 1979). This may account for the absence of the quartz intergrowths in the outer rims of the garnets in R229. These rims record pressures in excess of 8 kbars, but graphite is clearly still present in the assemblage. Alternatively, H_2O may be supplied in sufficient quantity to exhaust the buffer capacity of the graphite, via reaction (5). This could be achieved by either: (2) local dehydration reactions during prograde metamorphism or; (3) infiltration of an externally derived fluid. The growing garnet would then be subject to both the composition of the infiltrating fluid, and the liberation of local components rendered immobile in the presence of graphite buffered fluids.

A further example, again from Sulitjelma, in which one of these latter two processes would appear to have been operative, is worthy of special note. Although graphite is present as an included phase in garnet, it would appear to have been almost completely removed from the equilibrating bulk assemblage. The removal of graphite from the system occurred during garnet growth, and is recorded as an abrupt change in both the compositional and textural zonation, with the quartz intergrowths (and the sector-boundary inclusions) being absent from the outer zones of the garnet. The zoning profile of garnet G1-R238 is shown in fig. 6. The inner zone is characterized by an increase in Fe and Mg, and a decrease in Ca and Mn from the core to the interface with the outer zone. There is a hiatus in Fe at this point. The intergrowths are completely absent in the outer zone, although large irregular quartz inclusions are abundant. From this sharp inter-zone boundary to the outer rim of the garnet (a distance of approximately $200\ \mu\text{m}$) there is an increase in Ca and a decrease in Fe. Mg and Mn remain constant with the inner zone. The removal of graphite is thought to have arisen as a result of either local dehydration reactions or the sudden influx of an externally derived fluid, although in order to differentiate between these two processes additional observations are necessary.

Conclusion

Although the hypothesis proposed is completely general, the quantitative application of the theory involves some simplifications and assumptions that may affect the results. Specifically these include: (1) assuming that standard geothermometry and geobarometry will yield valid results where $P_{\text{H}_2\text{O}} < P_{\text{total}}$, and where, by implication, disequilibrium on a length scale of micrometres has been shown to

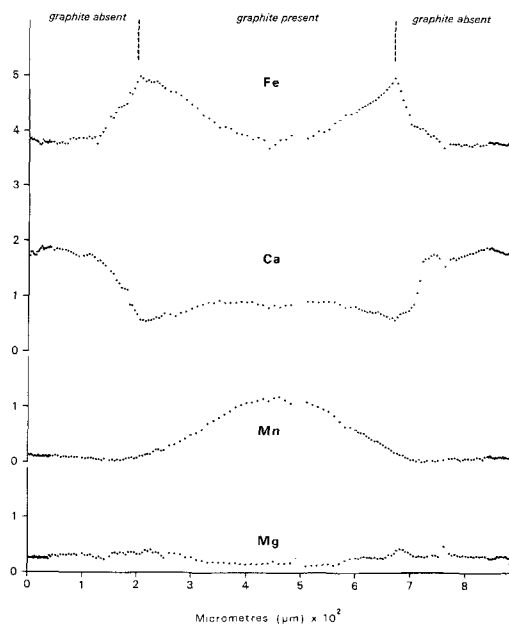


FIG. 6. Garnet zoning profiles for sample R238.

exist; (2) the use of ilmenite composition alone (using an independently determined T) in determining f_{O_2} ; (3) the choice of recalculation scheme used, (Powell and Powell, 1977); (4) the assumption that the Redlich-Kwong expression and the use of an ideal mixing model, truly approximate the behaviour of the fluid phase; (5) the paucity of data on element solubilities in mixed fluid compositions in the C-O-H system.

However, these uncertainties do not affect the major conclusions of this paper.

Further detailed studies are necessary before it is possible to generalize about the fluid conditions common to garnets containing this unusual inclusion and intergrowth pattern. The observations presented here demonstrate that the development of the quartz intergrowths is due to the presence of graphite in the assemblage. Graphite, by controlling the composition of the fluid effectively dictates both the mechanism and timing of garnet growth. However, the presence of garnets without such intergrowths in many graphite-bearing rocks indicates that this growth mechanism is not always operative. The results reported here may not be at variance with this observation, as solubilities sufficiently low for the intergrowths to develop may be restricted to a narrow range of P , T , and fluid composition space. Complete characterization of the fluid that coexists with these intergrowths, possibly utilizing fluid inclusions, may resolve this

problem. The theory outlined here may also be extended to account for the development of similar quartz intergrowths in a variety of other minerals, such as staurolite, chiastolite, and kyanite (Harker, 1939; Hollister and Bence, 1967; Hollister, 1969) as the presence of graphite is again the common factor in all such occurrences.

Acknowledgements. This study was supported by an NERC scholarship (GT4/83/GS/137). I would like to extend special thanks to G. D. Price for encouragement and assistance during the drafting of the text; M. F. Billet for making available the samples used; M. F. Miller for the calculation of fluid compositions; and G. A. Chinner for assistance with the Harker collection and for drawing my attention to the common development of such textures in garnet. I would also like to thank R. Mason, R. Hall, I. C. Young, P. D. Ballantyne, W. L. Kirk, W. Lamb, and S. A. Ross for helpful conversations and reviews.

REFERENCES

- Andersen, T. B. (1984) *Mineral. Mag.* **48**, 21–6.
 Billet, M. F. (1984) Ph.D. thesis. Univ. of London.
 Boyle, A. P., Hansen, T. S., and Mason, R. (1986) *Proc. Uppsala. Caledonide Symposium*. Wiley, New York (in press).
 Buddington, A. F., and Lindsley, D. H. (1964) *J. Petrol.* **5**, 310–57.
 Burton, W. K., Carbrera, N., and Frank, F. C. (1951) *Phil. Trans. R. Soc.* **243**, 299–358.
 Carmichael, D. M. (1970) *J. Petrol.* **11**, 147–81.
 Chalmers, B. (1964) *Principles of Solidification*. John Wiley, New York.
 Chinner, G. A. (1960) *J. Petrology*, **1**, 178–217.
 Eugster, H. P. (1959) In *Researches in Geochemistry* (P. H. Abelson, ed.) John Wiley & Sons, New York.
 Ferry, J. M., and Spear, F. S. (1978) *Contrib. Mineral. Petrol.* **66**, 113–18.
 Fisher, G. W. (1978) *Geochim. Cosmochim. Acta.* **42**, 1035–50.
 Frank, F. C. (1951) *Acta. Crystallogr.* **4**, 497–501.
 French, B. M. (1966) *Rev. Geophys.* **4**, 223–53.
 Frost, B. R. (1979) *Am. J. Sci.* **279**, 1033–59.
 Ghent, E. D., and Stout, M. Z. (1981) *Contrib. Mineral. Petrol.* **76**, 92–7.
 Greenwood, H. J. (1967) *Am. Mineral.* **62**, 1669–80.
 Harker, A. (1939) *Metamorphism*. 2nd edn., Methuen, London.
 Henley, K. J. (1970) *Nor. Geol. Tidsskr.* **50**, 97–136.
 Hodges, K. V., and Spear, F. S. (1978) *Am. Mineral.* **67**, 1118–34.
 Hollister, L. S. (1969) *Am. J. Sci.* **267**, 352–70.
 ——— and Bence, A. E. (1967) *Science*, **158**, 1053–6.
 Holloway, J. R. (1981) In *Short Course in Fluid Inclusions Applications to Petrology* (L. S. Hollister and M. L. Crawford, eds.)
 Kerrick, D. M. (1974) *Am. Mineral.* **59**, 729–62.
 Klapper, H. (1980) In *Characterization of crystal growth defects by X-ray methods* (B. K. Tanner and K. Bowen, eds.) Plenum Press, New York.
 Lamb, W., and Valley, J. W. (1984) *Nature*, **312**, 56–8.
 Loomis, T. P. (1982) *Can. Mineral.* **20**, 411–23.
 Miyashiro, A. (1964) *Geochim. Cosmochim. Acta*, **28**, 717–29.
 Novak, J. M., and Holdaway, M. J. (1981) *Am. Mineral.* **66**, 51–69.
 Novgorodov, P. G. (1975) *Geokhimiya*. no. 10, 1484–9.
 Ohmoto, H., and Kerrick, D. (1977) *Am. J. Sci.* **277**, 1013–44.
 Porter, D. A., and Easterling, K. E. (1981) *Phase Transformations in Metals and Alloys*. Van Nostrand, Reinhold.
 Powell, R., and Powell, M. (1977) *Mineral. Mag.* **41**, 257–63.
 Rumble, D. (1978) *J. Petrol.* **19**, 317–40.
 Rutter, J. W. (1958) *Liquid Metals and Solidification*. American Society for Metals.
 ——— and Chalmers, B. (1965) *Can. J. Phys.* **31**, 15–39.
 Shettel, D. L. (1973) *Eos*, **54**, 480.
 Skippen, G. B. (1977) In *Application of thermodynamics to petrology and ore deposits* (H. J. Greenwood, ed.) Mineral. Assoc. Can. Short Course Handbook, 66–83.
 Spry, A. (1969) *Metamorphic Textures*. Pergamon Press, Oxford.
 Thompson, J. B. (1970) *Geochim. Cosmochim. Acta.* **34**, 529–51.
 van Enckevort, W. J. P., Rosmalen, R. S. V., Klapper, H., and van der Linden, W. H. (1982) *J. Cryst. Growth*, **60**, 67–78.
 Walther, J. V., and Orville, P. M. (1983) *Am. Mineral.* **68**, 731–41.
 ——— and Wood, B. J. (1984) *Contrib. Mineral. Petrol.* **88**, 246–59.
 Woodsworth, G. J. (1977) *Can. Mineral.* **15**, 230–42.
 Yardley, B. W. D. (1977) *Am. Mineral.* **62**, 793–800.

[Manuscript received 18 October 1985;
 revised 21 February 1986]